A&A 452, 311–319 (2006)
DOI: 10.1051/0004-6361:20053869

Astronomy & Astrophysics

The intensity contrast of solar photospheric faculae and network elements

II. Evolution over the rising phase of solar cycle 23

A. Ortiz[1,⋆], V. Domingo[2], and B. Sanahuja[1]

[1] Departament d'Astronomia i Meteorologia, Universitat de Barcelona, Martí i Franquès 1, 08028 Barcelona, Spain
e-mail: Blai.Sanahuja@ub.edu
[2] Institut de Ciència dels Materials, Grupo de Astrofísica y Ciencias del Espacio, Universitat de València, 46071 València, Spain
e-mail: Vicente.Domingo-Codonyer@uv.es

Received 21 July 2005 / Accepted 9 January 2006

ABSTRACT

We studied the radiative properties of small magnetic elements (active region faculae and the network) during the rising phase of solar cycle 23 from 1996 to 2001, determining their contrasts as a function of heliocentric angle, magnetogram signal, and the solar cycle phase. We combined near-simultaneous full disk images of the line-of-sight magnetic field and photospheric continuum intensity provided by the MDI instrument on board the SOHO spacecraft. Sorting the magnetogram signal into different ranges allowed us to distinguish between the contrast of different magnetic structures. We find that the contrast center-to-limb variation (CLV) of these small magnetic elements is independent of time with a 10% precision, when measured during the rising phase of solar cycle 23. A 2-dimensional empirical expression for the contrast of photospheric features as a function of both the position on the disk and the averaged magnetic field strength was determined, showing its validity through the studied time period. A study of the relationship between magnetogram signal and the peak contrasts shows that the intrinsic contrast (maximum contrast per unit of magnetic flux) of network flux tubes is higher than that of active region faculae during the solar cycle.

Key words. Sun: activity – Sun: faculae, plages – Sun: magnetic fields

1. Introduction

The solar disk is a panoply of magnetic structures that form a hierarchy with a wide range of sizes, field strengths, and degrees of compactness (e.g. Schrijver & Zwaan 2000). The brightness signature of small magnetic features is a strong function of their heliocentric angle and their size; sunspots are dark while small flux tubes are generally bright. At high resolution, faculae consist of conglomerates of tightly packed unresolved bright points with diameters of about 100 km (Dunn & Zirker 1973; Keil & Muller 1983; Berger et al. 1995, 2004).

Two and a half decades of space-based monitoring of the total solar irradiance have revealed that it changes on time-scales ranging from minutes to the length of the solar cycle (Willson & Hudson 1988; Fröhlich & Lean 2004). Most of these variations arise from the changing presence and evolution of the aforementioned magnetic features. Variability on the solar rotation time-scale is associated with the passage of sunspots and faculae across the solar disk (e.g., Foukal & Lean 1986; Chapman 1987; Lawrence & Chapman 1990; Solanki & Fligge 2002). These variations can be as much as 0.3%. In addition, and superimposed on these variations, an 11-year cycle with a peak-to-peak amplitude on the order of 0.1% is now well established by recent total solar irradiance observations (Chapman 1987; Foukal & Lean 1988; Fröhlich 1994; Fröhlich & Lean 2004). Nowadays, there is a general trend towards accepting that surface magnetic features can account for most, if not all, of the solar-cycle irradiance variations (e.g., Solanki & Fligge 2002; Krivova et al. 2003; Walton et al. 2003; de Toma et al. 2004); see however, Kuhn et al. (1988) or Sofia (2004). In particular, the magnetic network has been pointed to as a large contributor to the solar-cycle variability. This important role has motivated us to study their radiative properties during the solar cycle.

In Ortiz et al. (2002), hereafter Paper I, we determined the contrast of small photospheric bright features – active region faculae and the network – as a function of both heliocentric angle and magnetogram signal, and we obtained an empirical function that predicts their contrast. The study was performed using data from ten days during 1999, so it did not consider any temporal evolution with the solar cycle. Now we consider one more variable – time – in order to analyze the solar cycle evolution of the contrast of these magnetic elements through the rising phase of cycle 23.

Facular and network contrasts are hard to measure, because they come from small bright points – often below the resolution limit – and with a very low contrast. In addition, their brightness signature is a function of their heliocentric angle, size, averaged magnetic field, wavelength, and spatial resolution (Solanki 1993, 1994). Therefore, it is difficult to compare observations made at different wavelengths, spatial resolutions, or field strengths. We combined cospatial and cotemporal photospheric intensity images and longitudinal magnetograms with the aim of accurately identifying magnetic features by their filling factor and of determining the contrast CLV of the different structures sorting them by their magnetic field. Such contrast measurements are expected to be useful not only for constraining models of flux tubes, but also for improving the modelling of solar

⋆ *Present address*: High Altitude Observatory, National Center for Atmospheric Research, PO Box 3000, Boulder, CO 80307-3000, USA, e-mail: ada@ucar.edu

Table 1. Characteristics of the selected images from 1996 to 2001. The MDI day (first column), date (second column), and UT time are given for the magnetograms ($t_{\rm mag}$, third column) and their corresponding averaged intensities ($t_{\rm int}$, fourth column).

MDI day	Date	$t_{\rm mag}$ (UT)	$t_{\rm int}$ (UT)	MDI day	Date	$t_{\rm mag}$ (UT)	$t_{\rm int}$ (UT)
1237	22/05/96	00:00	00:32	2225	04/02/99	03:11	03:11
1239	24/05/96	00:04*	01:18	2227	06/02/99	04:47	04:47
1249	03/06/96	12:48	12:44	2229	08/02/99	14:23	14:23
1296	20/07/96	22:28*	22:28	2292	12/04/99	11:12	10:31
1299	23/07/96	01:40*	01:40	2380	09/07/99	17:35	17:32
1313	06/08/96	16:00	16:02	2413	11/08/99	09:35	09:35
1389	21/10/96	19:11	19:12	2514	20/11/99	04:48	04:22
1407	08/11/96	19:12	18:56	2528	04/12/99	11:11	11:11
1416	17/11/96	11:15*	11:14	2529	05/12/99	11:11	11:11
1420	21/11/96	01:39*	01:27	2530	06/12/99	09:35	09:35
1502	11/02/97	06:27*	06:26	2583	28/01/00	17:35	17:27
1509	18/02/97	14:27*	14:26	2594	08/02/00	21:32	21:33
1529	10/03/97	17:36	17:19	2652	06/04/00	17:35	17:12
1538	19/03/97	00:00	00:08	2684	08/05/00	20:47	20:47
1572	22/04/97	11:16*	11:16	2693	17/05/00	20:48	21:01
1614	03/06/97	11:16*	11:16	2750	13/07/00	22:24	22:41
1701	29/08/97	03:15*	03:14	2751	14/07/00	00:00	00:01
1717	14/09/97	16:00	16:02	2804	05/09/00	19:11	19:11
1754	21/10/97	06:23	06:20	2860	31/10/00	17:35	17:43
1804	10/12/97	14:23	14:23	2890	30/11/00	21:47	21:44
1882	26/02/98	18:37	18:34	2973	21/02/01	19:11	18:56
1889	05/03/98	01:39*	02:02	3036	25/04/01	19:12	18:44
1944	29/04/98	12:47	12:47	3099	27/06/01	16:00	16:06
1963	18/05/98	11:11	11:11	3101	29/06/01	20:56	20:20
1968	23/05/98	06:23	06:23	3189	25/09/01	17:39*	18:01
1983	07/06/98	03:15*	02:30	3231	06/11/01	17:35	17:35
2000	24/06/98	11:11	11:11	3234	09/11/01	20:47	20:53
2130	01/11/98	11:11	11:11	3237	12/11/01	22:26	22:33
2131	02/11/98	06:23	06:23	3239	14/11/01	04:51*	05:30
2132	03/11/98	06:23	06:23	3252	27/11/01	20:47	20:47

* Indicates 5-min averaged magnetograms.

irradiance. Previous works were essentially photometric studies that did not distinguish features by their magnetic flux (Libbrecht & Kuhn 1984; Wang & Zirin 1987; Lawrence 1988; Lawrence & Chapman 1988; Steinegger et al. 1996; Walton et al. 2003; Ermolli et al. 2003); these works may suffer a bias towards brighter features. Relatively few contrast investigations that include the magnetogram signal can be found in the literature: for example, Frazier (1971), Foukal & Fowler (1984), Topka et al. (1992, 1997), Lawrence et al. (1993), or Paper I.

We analyzed the temporal evolution of the contrast of small bright features through the rising phase of cycle 23 (from 1996 to 2001), and continued working on the $\mu^2 - B^3$ model presented in Paper I. To carry out this investigation we used data from the MDI instrument on board SOHO (Domingo et al. 1995). It was necessary to perform a careful analysis of the detector's response during the studied period.

In Sect. 2 we present the data sets used and the analysis procedures. In Sect. 3 we describe the results of these investigations, which are discussed in Sect. 4. Finally, our conclusions are given in Sect. 5.

2. Data and analysis procedure

2.1. Data sets

The Solar Oscillations Investigation/Michelson Doppler Imager (SOI/MDI) instrument on board the SOHO spacecraft produces measurements of different observables in the Ni I 6768 Å absorption line. Narrow-band (94 mÅ) filtergrams are obtained at five tuning positions in the vicinity of the Ni I line by tuning the Michelson's peak transmission. The observables are computed from combinations of these five filtergrams. The solar image is projected onto a 1024×1024 CCD camera, and the pixel size is $2 \times 2''$. This state-of-the-art instrument is described in detail by Scherrer et al. (1995). Among the observables provided by MDI we are interested in both the full disk magnetograms and continuum intensity images. Magnetograms measure the line-of-sight component of the magnetic field averaged over the resolution element, $\langle |\boldsymbol{B}| \cos\gamma \rangle$, where γ is the angle between the magnetic field vector and the line-of-sight. For the sake of simplicity, we hereafter refer to $\langle |\boldsymbol{B}| \cos\gamma \rangle$ as B. The continuum intensity is a combination of the five mentioned filtergrams.

The MDI magnetograms are usually obtained every 96 min, except when 1-min cadence campaigns (for both magnetograms and continuum intensity images) are carried out. The analyzed data set consists of nearly simultaneous full-disk magnetograms and continuum-intensity images, recorded during 60 days (10 images per year) spread over the rising phase of solar cycle 23, and spanning from the 1996 minimum to 2001, around the solar maximum. These days were chosen because they contain everything from almost field-free quiet Sun periods to intense activity complexes; the sample contains magnetic activity spread over almost all $\mu = \cos\theta$ values. A detailed list of the selected data and their characteristics can be found in Table 1. We analyzed the temporal variation of the noise level in twelve series of the aforementioned 1-min cadence measurements (60 consecutive magnetograms measured during one hour, see Sect. 2.2).

2.2. Reduction method and analysis

We employed averages over 5 consecutive intensity images, taken at a cadence of 1 per minute, to reduce the noise and the signal of the p-mode oscillations in the intensity. Individual intensity images were first corrected for limb-darkening effects, as described in Paper I; then, each image was rotated to co-align it with the corresponding magnetogram before the averaging. Care was taken to use intensity images obtained as close in time to the magnetograms as possible. In all sixty cases but six, the two types of images were recorded within 30 min of each other, and only in one case was the time difference higher (74 min), because there were no intensities available closer in time to their corresponding magnetogram. Twenty-three out of the 60 image pairs were exactly simultaneous. Magnetograms are either 1 or 5-min averages, taken at a cadence of 96 min (see Sect. 2.2.1). Our final data sets are pairs of co-aligned averaged magnetograms and averaged photospheric continuum intensity images for each of the 60 selected days that can be compared pixel by pixel.

We determined the 1-σ noise level of the MDI magnetograms and continuum images as a function of position over the CCD array following the procedure described in Paper I, with some slight differences due to the fact that the present data sets cover half a solar cycle. A fundamental part of this work was to perform a careful study of the temporal dependence of the MDI sensitivity and stability. In Paper I we assumed that the MDI noise level was time independent and had remained unchanged between 1996 and 1999. Now we have derived the noise level of the magnetogram images for each year from 1996 to 2001.

We must calculate the temporal dependence of the instrumental noise itself, avoiding potential biases as much as possible due to the increasing solar activity; it is then imperative to remove any signature of solar activity. For this, we have compared subsequent averages derived from the twelve 1-min data sets of magnetograms spread over the six years. Specifically, we took 10 consecutive 1-min magnetograms from each data set and rotated them to the center of the time series to compensate for differential rotation. Then, we averaged two groups of five images each, grouping them into odds and evens. Magnetic activity over 40 G was removed from both averages. The next step was to subtract one 5-min average from the other, in order to remove magnetic activity as much as possible. Due to the minimal temporal differences between consecutive magnetograms, solar activity present in both averages should be approximately the same except for minimum changes in the magnetic configuration. After this subtraction the remaining fluctuations should be mainly instrumental fluctuations, i.e., noise. Finally, we applied the 100×100 pixels running box described in Paper I to derive the standard deviation of the MDI magnetograms as a function of position over the CCD array.

This process was carried out twice every year from 1996 to 2001 to evaluate the temporal change in the instrumental standard deviation. The resulting standard deviation surfaces, $\sigma_{\rm mag}(x, y)$, present an increase towards the SW limb, as discussed in Paper I. Figure 1 presents the temporal evolution of the noise level between 1996 and 2001 for the 5-min averaged magnetograms. The rounded-down average value is 8 G, with a variation of 8% over the six years; only a slight trend is visible in this time series, which means that the sensitivity of the detector remains almost constant with time. We chose the median of the two annual standard deviations as the noise level for that year, $\sigma^i_{\rm mag}$ (i stands for any of the six years). Note that the temporal variation of the instrumental noise could be even smaller because the calculated standard deviations may still contain some noise of solar origin due to magnetic fields that could have changed significantly within a few minutes.

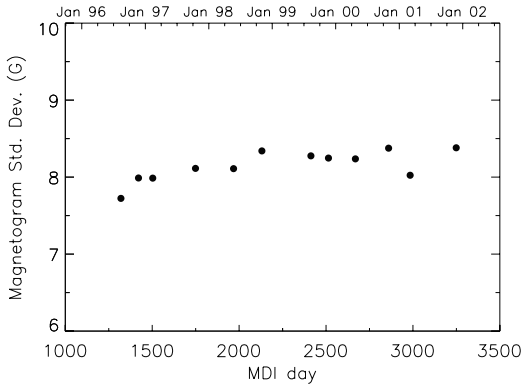

Fig. 1. Mean of the standard deviation surfaces (in Gauss) as a function of time, calculated twice every year between 1996 and 2001. Scatter is small and hardly any trend is visible.

We also analyzed the time evolution corresponding to the mean and standard deviation of the quiet Sun intensity, $\langle I_{\rm qs}\rangle$ and $\sigma_{\rm Iqs}$ respectively. The subscript qs denotes "quiet Sun". Pixels with an absolute magnetic signal value below 0.5 times $\sigma^i_{\rm mag}$ were considered as quiet Sun pixels. We evaluated the stability of the mean non-active Sun intensity with time for the 60 selected days following a procedure similar to that applied to magnetograms, finding that the intensity fluctuates around 2% through the analyzed period, thus also stable enough.

The surface distribution of solar magnetic features with a bright contribution to irradiance variations is identified by setting two thresholds to every magnetogram-intensity image pair. The first threshold looks for magnetic activity of any kind, and the second threshold masks sunspots and pores (see a more detailed explanation in Paper I). Isolated pixels were removed from the set. Then masks were constructed, for each selected day, that indicate the surface distribution of bright magnetic activity present over the solar disk at a given moment, as well as the associated contrast for each pixel (x, y), $C_{\rm fac}(x, y)$ (see definition in Eq. (1) of Paper I).

In Fig. 2 we show sample magnetograms (top), photospheric continuum intensities (middle), and their derived contrast masks (bottom) for two days during the rising phase of solar cycle 23. Only features lying above the given thresholds were pinpointed as black pixels; sunspots, for example, did not appear in the masks, but their surrounding faculae were identified. For each pixel selected by these masks, we obtained contrast, magnetic field strength averaged over the pixel, and position (represented by the heliocentric angle $\mu = \cos\theta$).

2.2.1. Magnetogram averages

The employed magnetograms are a mixture of 1-min and 5-min averages. According to Liu & Norton (2001), the noise level of MDI magnetic measurements is 16 G for 1-min magnetograms and 9 G for 5-min magnetograms, from which we take the 1.77 factor to convert between 1 and 5-min averages. This value does not agree with the expected value of 2.23 or $\sqrt{5}$, most probably implying that points below the noise level are not only instrumental noise, but some residuals of solar origin. Before flight the noise level of single 1-min MDI magnetograms had been

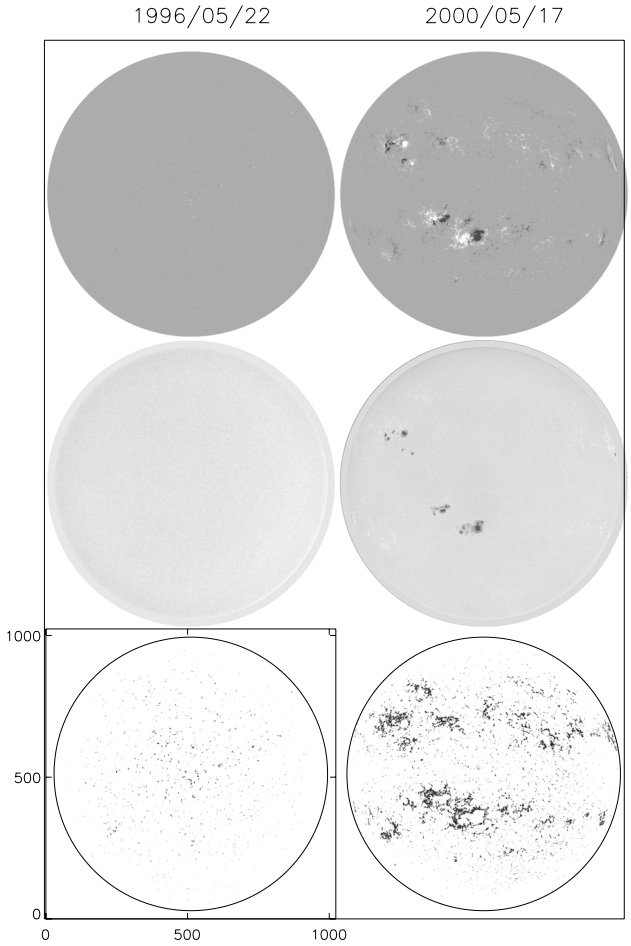

Fig. 2. Two examples of MDI magnetograms (*top panels*), their corresponding intensity images after limb-darkening removal (*middle panels*), and the resulting contrast masks (*lower panels*) for activity minimum (May 22, 1996, *left*) and maximum (May 17, 2000, *right*). A circle indicates the size of the Sun in each contrast mask.

estimated to be 20 G (Scherrer et al. 1995). After launch, this value was reduced to 14 G (Hagenaar 2001). We also derived this later value when performing the standard deviation procedure to single 1-min magnetograms, and so does Hagenaar (2001) by other means. Consequently, we assigned the derived noise level (8 G) whenever the magnetogram had an integration time of 5 min, and 1.77 times that noise (rounded down, 14 G) whenever the magnetogram represented a 1-min measurement.

3. Results

The contrast analysis performed here is similar to Paper I, except that now we extend it in time. We binned B/μ values into eight intervals that range from the threshold level, set at $3\sigma^i_{\rm mag}$, to 600 G; this threshold level is, on average, 24 G for 5-min measurements. Thus, we distinguish between the contrast CLV of magnetic features with different filling factors by sorting the magnetic flux into different bins. The first four intervals are slightly different than their equivalent in Paper I in order to account for the new threshold levels.

Figure 3 represents the contrast, $C_{\rm fac}$, as a function of μ for every B/μ interval during a period of solar minimum (1996). For each B/μ interval – but the last – a second degree polynomial least-squares has been fitted to guide the eye. Numbers in the upper left corner of each plot indicate the amount of pixels that belong to a given B/μ-bin. Figure 4 represents the same kind of dependence for a period of solar maximum (2001). To avoid overcrowding we binned data points; as the number of detected pixels grows up toward the solar maximum, the binning increases from sets of 20 points in 1996 to 40 points in 2001.

These figures, especially Fig. 4, reveal a clear evolution of the behavior of the contrast from one B/μ interval to another. Network features (top left panel) show a lower contrast, almost independent of μ. On the other hand, AR faculae (bottom panels) present a very pronounced CLV. Features with an intermediate magnetic signal show a gradual increase of the contrast towards the limb, as well as an increasingly pronounced CLV. Note the shift in the contrast peak towards lower values of μ for increasing values of B/μ. Low B/μ values (< 200 G) always report a positive contrast everywhere, while it becomes negative around disk center for $B/\mu \geq 200$ G.

By examining the temporal series of $C_{\rm fac}$ as a function of μ, it is easy to notice the increase in solar activity along the rising phase of the cycle (just looking at the number of pixels involved). While the highest B/μ bins at solar minimum just contain a few points, plots are overcrowded at solar maximum. For example, low magnetic signals ($B/\mu < 90$ G, most probably belonging to the network), multiply by 2.5 from 1996 to 2001, while high magnetic signals ($B/\mu > 400$ G, corresponding to strong faculae) increase by a factor of 70. This is a direct consequence of the growing number of active regions present over the solar disk as solar maximum approaches.

Following the method detailed in Paper I, we performed a multivariate analysis in order to obtain an empirical expression for the contrast of photospheric features, both as a function of μ and magnetogram signal, $C_{\rm fac}(\mu, B/\mu)$. In this work we extend the analysis through the rising phase of solar cycle 23. Again, a $(\mu, B/\mu)$ grid is used, where grid dimensions are $0.1 \leq \mu \leq 1$ and $24\,{\rm G} \leq (B/\mu) \leq 630\,{\rm G}$. The μ values have been binned linearly, with $\Delta\mu = 0.1$. The B/μ bins were chosen to be equally spaced on a logarithmic scale, with $\Delta \log(B/\mu) = 0.05$, in order to compensate for the fact that magnetic signals are mostly concentrated towards lower values (Figs. 3 and 4). We used the fitting function applied in Paper I (a second-order polynomial function of μ and a cubic function of B/μ), with the contrast constrained to go through zero when $B/\mu = 0$, which is the expected behavior for the quiet Sun. The terms of the expression for the contrast $C_{\rm fac}(\mu, B/\mu)$ can be grouped as:

$$\begin{aligned} C_{\rm fac}(\mu, B/\mu) \;=\; & \left[a_{01} + a_{11}\mu + a_{21}\mu^2\right]\left(\frac{B}{\mu}\right) \\ & + \left[a_{02} + a_{12}\mu + a_{22}\mu^2\right]\left(\frac{B}{\mu}\right)^2 \\ & + \left[a_{03} + a_{13}\mu + a_{23}\mu^2\right]\left(\frac{B}{\mu}\right)^3 \end{aligned} \qquad (1)$$

where a_{ji} are the coefficients of the fit for each year and are given in Table 2. The result of these fits for each of the six years are surfaces that represent the contrast of bright features. The validity of Eq. (1) is limited by the MDI parameters, such as wavelength and spatial resolution, 6768 Å and 2″, respectively. Other values of these parameters would result in different contrast dependences on μ and B/μ.

As can be seen in Figs. 3 and 4, it appears that the contrast CLV of small magnetic features does not change significantly with time. To quantitatively verify this impression, we performed a Student's-t test to compare the contrasts for different years relative to the contrast during the activity minimum of

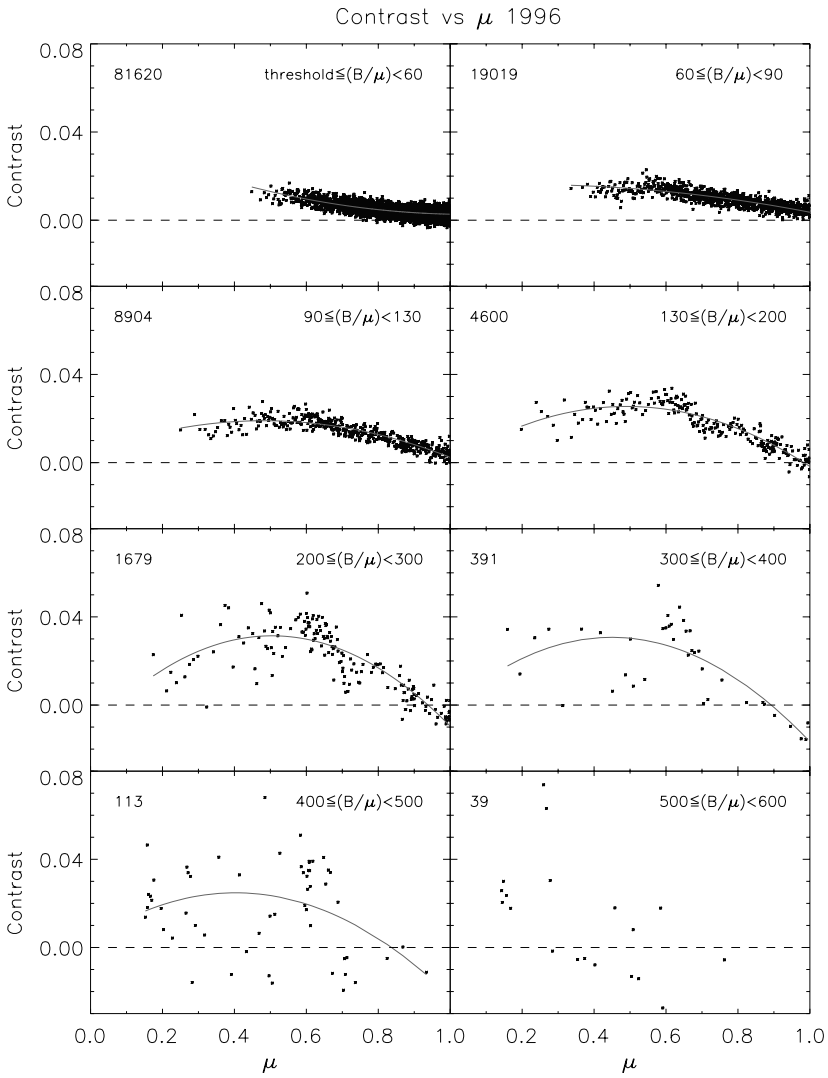

Fig. 3. Facular and network contrast at solar minimum (1996) as a function of μ for eight magnetic field intervals, from network values (*top left panel*) to strong faculae (*lower right*). A dashed line indicates $C_{\rm fac} = 0$. Solid curves represent a second-degree polynomial least-square fit to the points; $\mu = 1$ is the disk center, $\mu = 0$ is the limb. The number in the upper left corner counts the number of pixels in each B/μ interval.

1996. We calculated cuts to the yearly contrast surfaces in both variables, μ and B/μ, and found that the absolute differences between the contrast for 1997, 1998, 1999, 2000, and 2001 with respect to the minimum are smaller than 0.01, being the relative differences smaller than 10% (the higher values appear near the limb and are due to the associated foreshortening). Figure 5 shows two examples of these differences between different years with respect to 1996. These examples correspond to some B/μ intervals shown in Figs. 3 and 4, and are representative of the contrast comparison for $C_{\rm fac}(\mu)$ and $C_{\rm fac}(B/\mu)$ (left and right panels, respectively). The Student's-t test reveals that, at the 95% confidence level, there is no significant difference between contrast means for different years, and the one during activity minimum. Moreover, these differences are neither arranged in any specific temporal order nor do they follow any pattern, as can be seen in Fig. 5. In order to compare these differences among contrasts, Table 3 presents the calculated t-values that result from the test, for the same magnetic flux bins as shown in Figs. 3 and 4. The tabulated t-value (for 16 degrees of freedom) and probability $p = 0.05$ (95% confidence level) is 2.12. Therefore we conclude that, with a 10% precision, there is no temporal trend for the contrast CLV. Since the nature of the observed contrasts is related to the structure of the underlying flux tubes, this supports the idea that the physical properties of the facular flux tubes do not vary with time, in particular with the solar cycle.

The dependence of the peak of $C_{\rm fac}$ on B/μ is shown in Fig. 6. This figure is similar to Fig. 8 in Paper I, but this time we consider the temporal evolution of the small photospheric magnetic elements. Different symbols are representative of different years. For each year, the μ-values at which $C_{\rm fac}$ peaks are plotted against the corresponding magnetic signal in Fig. 6a. Figure 6b shows the maximum $C_{\rm fac}$ values, $C_{\rm fac}^{\rm max}$, plotted as a function of B/μ. These maximum contrasts are derived from the corresponding modeled surfaces. Finally, Fig. 6c shows $C_{\rm fac}^{\rm max}/(B/\mu)$ represented as a function of B/μ, where $C_{\rm fac}^{\rm max}/(B/\mu)$ is the specific contrast (maximum contrast per unit magnetic flux). Errors in μ and $C_{\rm fac}^{\rm max}$ are estimated from the difference between the peak of the fitted surfaces and the peak obtained directly from the data points. Error bars plotted in Fig. 6 represent an average over the annual errors. Figure 6c proves that the contrast per unit of magnetic signal decreases with an increasing magnetic signal. Individual flux tubes cannot be resolved by MDI pixels, therefore we cannot infer their intrinsic contrast from Fig. 6b. However, by normalizing by B/μ, we obtain a magnitude roughly proportional to the intrinsic brightness of the elemental flux tubes, assuming that the field strength of the elemental magnetic flux tubes lies in a narrow range. Figure 6 (especially Fig. 6b) also reflects that contrasts do not change significantly along the present solar cycle. Notice that these results apply to the intensity of the continuum measured at the Ni I 6768 Å line

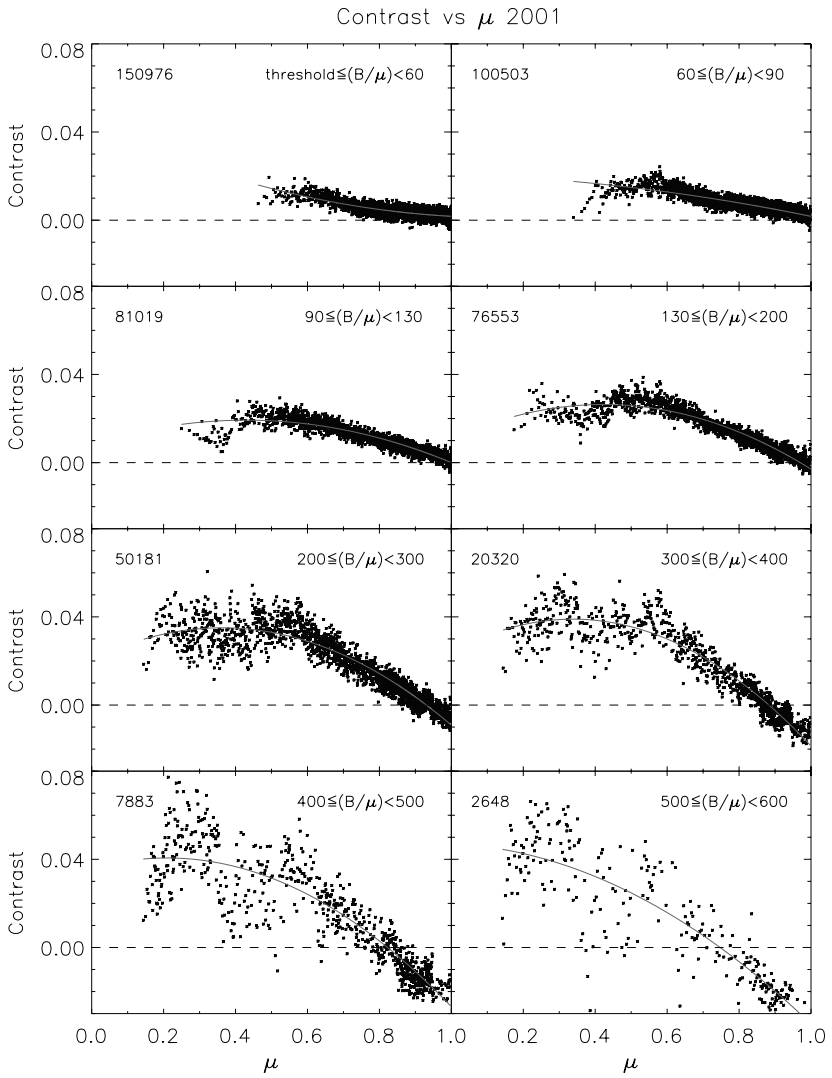

Fig. 4. Same as Fig. 3 for a solar maximum period (2001).

Table 2. Coefficients $a_{j,i}$ of the multivariate fits corresponding to each of the six years.

Year	a_{01} ($\times 10^{-4}$)	a_{11} ($\times 10^{-4}$)	a_{21} ($\times 10^{-4}$)	a_{02} ($\times 10^{-6}$)	a_{12} ($\times 10^{-6}$)	a_{22} ($\times 10^{-6}$)	a_{03} ($\times 10^{-10}$)	a_{13} ($\times 10^{-10}$)	a_{23} ($\times 10^{-10}$)
1996	−1.64	11.62	−9.18	1.219	−2.721	0.638	−24.36	15.01	22.91
1997	−2.04	13.86	−11.45	1.933	−6.385	4.033	−33.97	83.00	−43.84
1998	−1.61	11.71	−9.56	1.440	−4.363	2.454	−19.58	41.10	−16.45
1999	−2.18	12.08	−9.31	0.646	−1.753	0.609	−2.22	−6.31	13.12
2000	−1.81	12.87	−10.73	0.751	−2.972	1.822	−6.64	16.02	−5.68
2001	−0.37	8.98	−8.34	0.538	−2.520	1.660	−5.84	15.38	−6.45

with a pixel size of 2″ and a resolution of 4″. There are indications (Domingo et al. 2005) that the maximum contrast is found at lower values of μ when the measurements are performed with higher resolution.

A comparison of Figs. 3 and 4 above and Fig. 3 in Paper I shows that there are some differences in the CLV of the contrast. The contrasts obtained in Paper I are systematically higher and show a different contrast CLV behavior for low B/μ fluxes. These differences are due to the fact that in Paper I a common quiet Sun intensity background was used, while in the present study the non-active Sun backgrounds are calculated individually for every observed day. To prove it, we recalculated the contrasts shown in Paper I with the quiet Sun background used there, as well as with individual quiet Sun backgrounds, obtaining the same observed differences.

4. Discussion

4.1. Comparison with previous observations

According to Pap & Fröhlich (2002), it is not known whether the contrast of the network changes as a function of wavelength, position on the disk, and phase in the solar cycle. This is precisely the topic addressed in this work. We have seen that the contrast of small flux tubes – those producing a bright contribution to the total irradiance – depends on their position on the visible disk and on the magnetic flux, but do not vary with time.

Comparison with other contrast center-to-limb observations is not easy because of the differences in the selected wavelength, spatial resolution, range of studied heliocentric angles, magnetic filling factor, and size of the analyzed features. All these factors

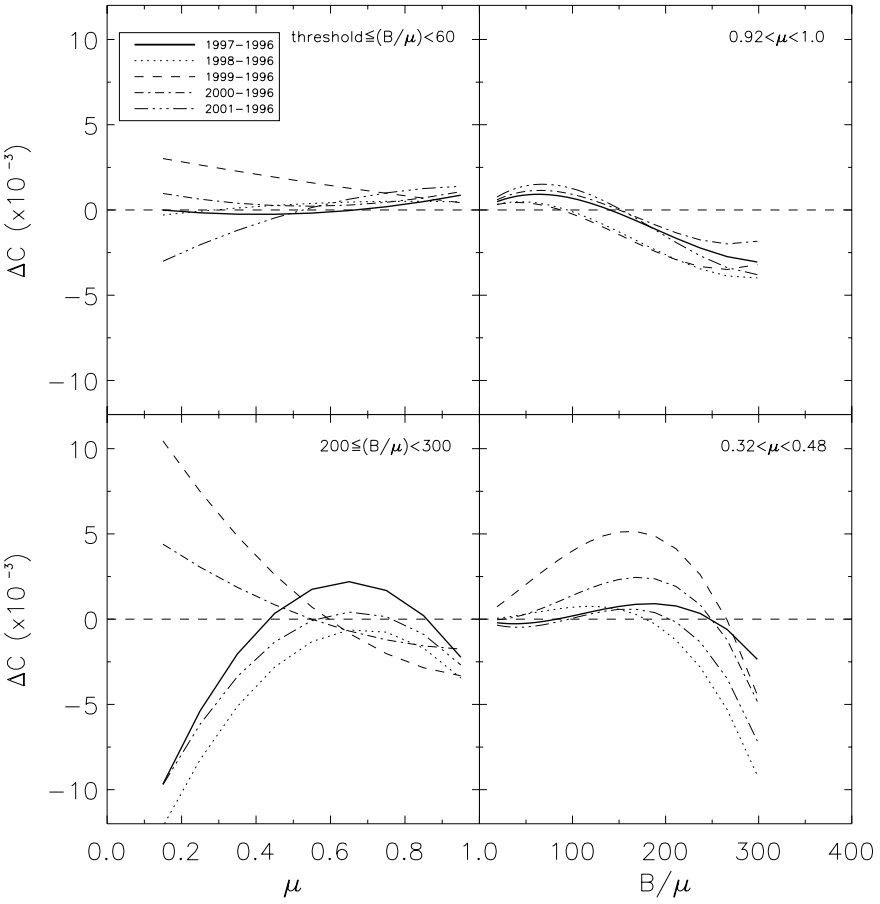

Fig. 5. Differences of yearly contrasts respect to the 1996 contrast as a function of μ (left column) and as a function of B/μ (right column), for sample magnetic field ranges and positions over the solar disk. Each curve represents the difference, for each year, between the calculated contrast from Eq. (1) and the 1996 contrast, in order to search for contrast changes relative to the activity minimum.

Table 3. Computed t-values from the comparison of the contrast for different years with respect to the activity minimum contrast (1996, otherwise indicated), for the B/μ bins shown in Figs. 3 and 4.

B/μ	1997	1998	1999	2000	2001
< 60 G	0.05	0.21	1.18	0.40	0.21
60 – 90 G	0.07	0.18	1.24	0.52	0.11
90 – 130 G	0.07	0.10	1.24	0.59	0.05
130 – 200 G	0.03	0.22	0.99	0.52	0.10
200 – 300 G	0.43	1.02	0.02	0.19	0.77
300 – 400 G*	-	1.01	0.30	0.27	0.81
400 – 500 G**	-	-	0.12	0.20	0.30
500 – 600 G**	-	-	0.63	0.40	0.09

* Comparison with respect to 1997; ** Comparison with respect to 1998.

contribute to the scatter between the existing contrast measurements. Our results differ from earlier observations of the contrast of bright features, especially when considering magnetic signals $B/\mu > 200$ G at disk center. Previous measurements of disk center facular contrasts have frequently yielded positive values, while in Paper I we measured negative contrasts at disk center for faculae within the range $200 < B/\mu < 600$ G, as did, for example, Topka et al. (1992, 1997) or Lawrence et al. (1993) at other spatial resolutions and wavelengths. In this work we show that this is still true at different phases of solar activity. Measuring the contrast at disk center is particularly important because it helps in determining the thermal structure of the deep layers.

The variation in the contrast of small magnetic features with the solar cycle has hardly been investigated. To our knowledge, only Ermolli et al. (2003) and this work address this problem at the photospheric level. These authors use Rome-PSPT images

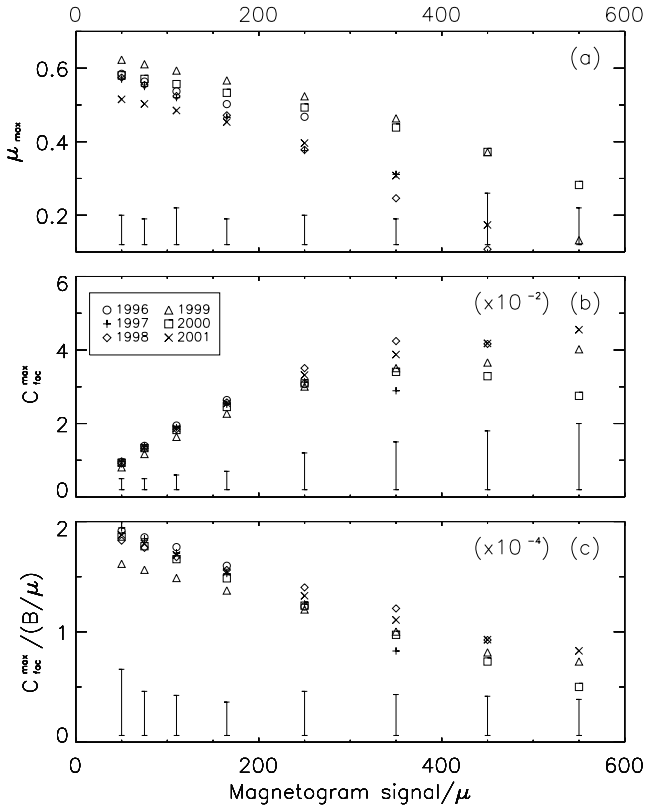

Fig. 6. Dependence on the corrected magnetic flux per pixel, B/μ, of: **a)** $\mu_{\max}$; **b)** $C_{\rm fac}^{\max}$ times 10^2; **c)** $C_{\rm fac}^{\max}/(B/\mu)$ times 10^4. Each symbol is representative of a different year (see legend). Error bars represent an average over the annual errors; for clarity, they have been shifted down.

to analyze the quiet network pattern during the current solar cycle and report a network contrast change of about 0.05% during that period of time. A possible explanation for the discrepancy with the results presented here is that their identification method differs substantially from ours: they only use photometric intensity images, while we combine magnetograms with intensity images to search for the desired features. Thus, different selection criteria yield to different considerations of what the network is. In addition, they restrict their work to the quiet network pattern, while we consider a broader population of small magnetic elements. In particular, the contrast change identified by these authors can be due to a change in the distribution of elements within the network component with the solar cycle or, similarly, to an increase in the filling factor of their selected pixels from minimum to maximum; as the maximum is approached, more network tubes would be included within a pixel, increasing the brightness of such pixel. Also, our 10% precision could well include the small change that these authors report. At the chromospheric level, Worden et al. (1998) also find that the intensity contrasts of the plage, enhanced network, and active network remain approximately constant over the solar cycle.

It is remarkable that an expression as given by Eq. (1) reproduces the dependence of the contrast of bright features on their position (μ) and on the magnetic flux per pixel (B/μ), within the range $0.1 \leq \mu \leq 1$ and $24\,\mathrm{G} \leq (B/\mu) \leq 630\,\mathrm{G}$. A relative accuracy of better than 12% is achieved almost everywhere within this domain and in the period studied. We are aware that more work needs to be done, since other parameters on which the contrast depends are kept fixed, such as spatial resolution and wavelength. The $\mu^2 - B^3$ description of the facular and network contrast has proved valid for different phases of the present solar cycle and degrees of solar activity, and can be introduced as one input into different models that reproduce the facular irradiance (see, e.g., Lockwood 2005). Ideally, models that reproduce the facular contribution to the total solar irradiance variations should rely on broadband photometric observations of the facular contrast. However, almost every facular contrast measurement found in the literature is monochromatic. Foukal et al. (2004) have recently shown that this problem can be circumvented by applying a blackbody correction to monochromatic facular contrasts, thus converting such measurements a posteriori into bolometric contrasts.

4.2. Theoretical considerations

We have shown that the intensity contrast of small photospheric magnetic elements is time independent during the studied period. Since the nature of the observed contrast CLV is directly related to the structure of the flux tubes making up these magnetic elements, this observed invariance with time supports the idea that the physical properties of the facular flux tube do not vary with time, in particular with the solar cycle. This temporal invariability has often been assumed in the past – there is no theoretical argument that implies that small magnetic features should have a different structure at solar minimum than at maximum – but has never before been verified. Interestingly enough, Albregtsen et al. (1984) report that the umbra contrast is a linear function of the phase in the solar cycle, yielding changes in the contrast of sunspots of around 30% along the cycle. Such a temporal change should have been detected with the precision achieved here; however, small magnetic elements seem to present a different behavior along the solar cycle than sunspots, as seen in this work.

If the contrast of the studied features does not vary with time, a possible explanation to the increase in the solar irradiance during solar activity maximum (or for the increase in the contrast found by Ermolli et al. 2003) is the large increase in the number of features at solar maximum. The ratio between the number of magnetic features at maximum relative to that at minimum increases with B/μ or, alternatively, with the size of the structure. For example, from Figs. 3 and 4 we found that features with $B/\mu < 90$ G increased by a factor of 2.5 from 1996 to 2001. Meunier (2003) finds a factor of 2.9 for fluxes below 3×10^{19} Mx, which approximately correspond to network patches. High magnetic signals ($B/\mu > 400$ G) increased by a factor of 70 from 1996 to 2001, as a direct consequence of the growing number of active regions present over the disk when reaching the maximum.

The upper panels of Figs. 3 or 4 refer to, on average, small flux tubes that dominate the network population, while the lower panels of those figures refer to the larger tubes mostly present in AR faculae. There are clear differences between small network flux tubes and tubes found in AR faculae, i.e. regions with larger B/μ. Network tubes are bright everywhere on the solar disk and exhibit a low contrast (Fig. 6b) but a high specific contrast (Fig. 6c). Somewhat larger tubes are predicted to appear dark at disk center but bright near the limb (Knölker & Schüssler 1988); we can see this behavior in the lower panels of Fig. 4. Their contrast is higher than for smaller tubes (Fig. 6b) but show a lower specific contrast (Fig. 6c). This behavior for the specific contrast was already shown in Paper I, but here we extend its validity for the rising phase of solar cycle 23; and there is no reason to think that this will change through the remaining solar cycle. This observed behavior implies that network flux tubes are intrinsically brighter than AR flux tubes along the solar cycle. The greater brightness at disk center implies that network flux tubes may have a hotter bottom than larger flux tubes, which follows directly from Figs. 3 and 4 and was predicted by Spruit (1976). Another difference between network and facular populations is that the higher the magnetic signal, the lower the μ-value at which the contrast peaks (see Fig. 6a), so that network-like features dominate at disk center and features with larger B/μ closer to the limb. This is true for the studied period.

Finally, the high specific contrast of small B/μ features (Fig. 6c) during the solar cycle, and the fact that their contrast is positive over the whole solar disk (i.e. at all μ's), makes us think that a change in the distribution of the network – for example with the solar cycle – makes a significant contribution to the change of the total solar irradiance (see, e.g., Fröhlich & Lean 2004). Since the contrast CLV is an input for some models that reproduce the facular contribution to irradiance variations, and we have shown that the $\mu^2 - B^3$ empirical description for the facular contrast is valid along the solar cycle, this description can in principle be used to reproduce irradiance variations for any time within the present solar cycle (Wenzler et al. 2002; Lockwood 2005), at least up to 10% precision.

5. Conclusions

We have presented an analysis of the intensity contrast of small bright magnetic elements – from AR faculae to the network – and its dependence on position, magnetic field strength, and phase of the solar cycle using MDI/SOHO data. These magnetic features can play an important role in the solar cycle irradiance variations, which are not fully understood.

While in Paper I we showed that the contrast CLV of magnetic features changes gradually with magnetogram signal,

we show here that this behavior for $C_{\rm fac}(\mu)$ remains during the solar cycle. Our results indicate that the contrast of small bright features does not present a temporal dependence with solar cycle phase, with an uncertainty of 10%. From this result we infer that the physical properties of the underlying flux tubes do not vary with time.

The validity of the simple expression presented in Eq. (1) – the $\mu^2 - B^3$ model to predict the contrast of bright features – has been extended to the rising phase of solar cycle 23.

We have shown that the intrinsic contrast of network flux tubes is higher than that of AR faculae during the solar cycle; moreover, the network always makes a positive contribution to the irradiance. Therefore, it is reasonable to conclude that any change in the network distribution may have a significant impact on the variation of the total irradiance.

Finally, we conclude that a very careful analysis of the response of the detector with time is imperative in any study of the long-term radiative properties of faculae and the network. It is essential to accurately determine the quiet Sun intensity backgrounds and noise levels.

Next steps in this investigation would include, but would not be limited to, introducing the $\mu^2 - B^3$ model (corrected for bolometric measurements) in reproductions of the solar cycle irradiance variations, and separating the contributions from faculae, network, and other magnetic structures in order to analyze the relative role of each of them. Of special interest would be to compare the role of AR faculae and the network in these long-term irradiance variations.

Acknowledgements. Part of this work was supported by the Spanish Ministry of Science and Technology through project AYA2001-3304 and AYA2004-03022. AO acknowledges financial support from the DURSI (Generalitat de Catalunya) grant 2001 TDOC00021. S. Criscuoli is acknowledged for helpful discussions. We thank the referee for valuable comments that led to the improvement of the manuscript.

References

Albregtsen, F., Joràs, P. B., & Maltby, P. 1984, Sol. Phys., 90, 17
Berger, T. E., Schrijver, C. J., Shine, R. A., et al. 1995, ApJ, 454, 531
Berger, T. E., Rouppe van der Voort, L. H. M., Löfdahl, M. G., et al. 2004, A&A, 428, 613
Chapman, G. A. 1987, ARA&A, 25, 633
de Toma, G., White, O., Chapman, G., et al. 2004, ApJ, 609, 1140
Domingo, V., Fleck, B., & Poland, A. I. 1995, Sol. Phys., 162, 1
Domingo, V., Ortiz, A., Sanahuja, B., & Cabello, I. 2005, Adv. Space Res., 35, 345
Dunn, R. B., & Zirker, J. B. 1973, Sol. Phys., 33, 281
Ermolli, I., Berrilli, F., & Florio, A. 2003, A&A, 412, 857
Foukal, P., & Fowler, L. 1984, ApJ, 281, 442
Foukal, P., & Lean, J. L. 1986, ApJ, 302, 826
Foukal, P., & Lean, J. L. 1988, ApJ, 328, 347
Foukal, P., Bernasconi, P., Eaton, H., & Rust, D. 2004, ApJ, 611, L57
Frazier, E. N. 1971, Sol. Phys., 21, 42
Fröhlich, C. 1994, in The Sun as a Variable Star: Solar and Stellar Irradiance Variations, ed. J. Pap, C. Fröhlich, H. S. Hudson, & S. K. Solanki (Cambridge: Cambridge Univ. Press), IAU Coll., 143, 28
Fröhlich, C., & Lean J. L. 1998, Geophys. Res. Lett., 25, 4377
Fröhlich, C., & Lean, J. L. 2004, A&ARv, 12, 273
Hagenaar, H. J. 2001, ApJ, 555, 448
Keil, S. L., & Muller, R. 1983, Sol. Phys., 87, 243
Knölker, M., & Schüssler, M. 1988, A&A, 202, 275
Krivova, N. A., Solanki, S. K., Fligge, M., & Unruh, Y. C. 2003, A&A, 399, L1
Kuhn, J. R., Libbrecht, K. G., & Dicke, R. H. 1988, Science, 242, 908
Lawrence, J. K. 1988, Sol. Phys., 116, 17
Lawrence, J. K., & Chapman, G. A. 1988, ApJ, 335, 996
Lawrence, J. K., & Chapman, G. A. 1990, ApJ, 361, 709
Lawrence, J. K., Topka, K. P., & Jones, H. P. 1993, J. Geophys. Res., 98, 18911
Libbrecht, K. G., & Kuhn, J. R. 1984, ApJ, 277, 889
Liu, Y., & Norton, A. A. 2001, SOI Technical Note SOI TN-01-144 (Stanford: Stanford University)
Lockwood, M. 2005, Solar Outputs, Their Variations and Their Effects on Earth, In Saas-Fee Advanced Course 34, The Sun, Solar Analogs and the Climate, ed. I. Rüedi, M. Güdel, & W. Schmutz (Berlin: Springer), 273
Meunier, N. 2003, A&A, 405, 1107
Ortiz, A., Solanki, S. K., Domingo, V., Fligge, M., & Sanahuja, B. 2002, A&A, 388, 1036 (Paper I)
Pap, J., & Fröhlich, C. 2002, Adv. Space Res., 29, 1571
Scherrer, P. H., Bogart, R. S., Bush, R. I., et al. 1995, Sol. Phys., 162, 129
Schrijver, C. J., & Zwaan, C. 2000, in Cambridge Astrophysics Series 34, Solar and Stellar Magnetic Activity (Cambridge: Cambridge Univ. Press)
Sofia, S. 2004, EOS Trans. (American Geophysical Union), 85, 217
Solanki, S. K. 1993, Space Sci. Rev., 63, 1
Solanki, S. K. 1994, in The Sun as a Variable Star: Solar and Stellar Irradiance Variations, ed. J. Pap, C. Fröhlich, H. S. Hudson, & S. K. Solanki (Cambridge: Cambridge Univ. Press), IAU Coll., 143, 226
Solanki, S. K., & Fligge, M. 2002, Adv. Space Res., 29, 1933
Spruit, H. C. 1976, Sol. Phys., 50, 269
Steinegger, M., Brandt, P. N., & Haupt, H. F. 1996, A&A, 310, 635
Topka, K. P., Tarbell, T. D., & Title, A. M. 1992, ApJ, 396, 351
Topka, K. P., Tarbell, T. D., & Title, A. M. 1997, ApJ, 484, 479
Walton, S. R., Preminger, D. G., & Chapman, G. A. 2003, ApJ, 590, 1088
Wang, H., & Zirin, H. 1987, Sol. Phys., 110, 281
Wenzler, T., Solanki, S. K., Fluri, D. M., et al. 2002, in ESA SP-508, SOHO 11: From Solar Min to Max, Half a Solar Cycle with SOHO, (Noordwijk: ESA Publications Division), 231
Willson, R. C., & Hudson, H. S. 1988, Nature, 332, 810
Worden, J., White, O., & Woods, T. 1998, ApJ, 496, 998